Measurement of the linear electro-optic coefficients of sol-gel derived strontium barium niobate thin films using a two-beam polarization interferometer

Junmo Koo, Changho Lee, Jae Hyeok Jang, Kwangsoo No, and Byeong-Soo Bae[a)]
Laboratory of Optical Materials and Coating (LOMC), Department of Materials Science and Engineering, Korea Advanced Institute of Science and Technology (KAIST), Taejon 305-701, Korea

(Received 17 November 1999; accepted for publication 7 March 2000)

A two-beam polarization interferometer in a reflection configuration is used to measure the electro-optic coefficients of highly oriented strontium barium niobate thin films prepared by a sol-gel method. The technique enables the determination of the electro-optic coefficients of films using a strong Fabry–Perot effect with automatic adjustment and maintenance of the operation point of the interferometer. The linear electro-optic coefficients increase with increasing Sr content in the films. © *2000 American Institute of Physics.* [S0003-6951(00)01018-4]

Strontium barium niobate, $Sr_xBa_{1-x}Nb_2O_6$ (denoted $SBN_x \cdot 100$), where $0.25 \leqslant x \leqslant 0.75$, is currently being investigated as a potential material for many microdevice applications such as pyroelectric infrared detectors, piezoelectrics, electro-optic modulators, and holographic storages.[1,2] Specifically, it has a much larger electro-optic coefficient than other ferroelectric materials such as $LiNbO_3$, $LiTaO_3$, and KH_2PO_4(KDP),[3,4] and preparation of epitaxial thin films of SBN is important for optical waveguide applications. There have been just a few reports on the growth of SBN thin films using different techniques.[5–7] Among these techniques, sol-gel methods have been developed for ferroelectric thin film processing due to excellent homogeneity, ease of chemical composition control, high purity, low processing temperature, and film uniformity over a large area. However, there has not been any reported effort in the measurements of electro-optic coefficients in sol-gel derived SBN thin films. Although a few reports on electro-optic coefficients of SBN thin films prepared by pulsed laser deposition (PLD) have been made,[8,9] the film composition is restricted to high Sr contents ($x=0.6$ and 0.75) and the composition dependence has not been studied. Since the Curie temperature of SBN material increases as the Sr content decreases,[1] SBN thin films with low Sr content and high Curie temperature may promise the fabrication of reliable waveguides. In this letter, we measured high electro-optic coefficients r_{33} of SBN thin films with various compositions prepared by a sol-gel method, using a new technique with a two-beam polarization (TBP) interferometer.

Four compositions were investigated in the present study with $x=0.25$, 0.40, 0.60, and 0.75. Strontium metal, barium metal, and niobium ethoxide were used as the starting reagents. 2-methoxyethanol was used as a solvent to avoid precipitation. A precise procedure for preparing the precursor solution is presented in another paper.[10] The solution was spin coated onto Pt(100)/MgO(100) substrates at 2000 rpm for 30 s. After air drying, the film was dried on a hot plate at 180 °C for 10 min and 360 °C for 10 min, to remove organic residues completely. These films were then heat treated at 900 °C by a modified heating schedule to enhance densification and crystallization.[10] Figure 1 shows the x-ray diffraction (XRD) patterns of SBN thin films (6000 Å) on Pt(100)/MgO(100) substrates as a function of film composition. All of the crystallized films have the *c*-axis preferred orientation, regardless of composition. Generally, SBN films on MgO(100) substrates are known to grow in the *c*-axis orientation.[6–10] Because the lattice parameter of the Pt unit cell is similar to that of MgO,[11] the films on Pt(100)/MgO(100) substrates have the same orientation.

The electro-optic coefficients of SBN thin films were measured using a TBP interferometer. The basic idea with polarization interferometry is to use the electric field induced phase-shift difference between the *s*- and *p*-polarized beams transmitted through the film, then reflected from the opposite surface of the film.[12] When the incident laser beam is reflected from a Pt electrode on the thin film (Fig. 2), the phase-shift φ_{2sp} between *s*- and *p*-polarized waves for a poled film is given by

$$\begin{aligned}\phi_{2sp} &= \left(\frac{4\pi d}{\lambda}\right)\left[\frac{n_s}{\cos\alpha_s} - \frac{n_p}{\cos\alpha_p} - \sin\theta(\tan\alpha_s - \tan\alpha_p)\right] \\ &= \left(\frac{4\pi d}{\lambda}\right)\left[\frac{(n_s - \sin\theta\sin\alpha_s)}{\cos\alpha_s} - \frac{(n_p - \sin\theta\sin\alpha_p)}{\cos\alpha_p}\right] \\ &= \left(\frac{4\pi d}{\lambda}\right)[(n_s^2 - \sin^2\theta)^{1/2} - (n_p^2 - \sin^2\theta)^{1/2}] \\ &= \left(\frac{4\pi d}{\lambda}\right)\left[(n_o^2 - \sin^2\theta)^{1/2} - \left(\frac{n_o}{n_c}\right)(n_c^2 - \sin^2\theta)^{1/2}\right],\end{aligned} \tag{1}$$

where θ is the incidence angle of the laser beam, d is the thickness of the film, α_s and α_p are the refraction angles of the *s*- and *p*-polarized waves in the film, n_s and n_p are the refractive indices of the anisotropic film for the optical field components perpendicular (*s*-polarized wave) and parallel (*p*-polarized wave) to the plane of incidence, n_o and n_e are the ordinary and extraordinary refractive indices, respectively, and λ is the wavelength. The phase change under an electric field with small ac amplitude, E_m, is given by

[a)]Electronic mail: bae111@rsphy1.anu.edu.au

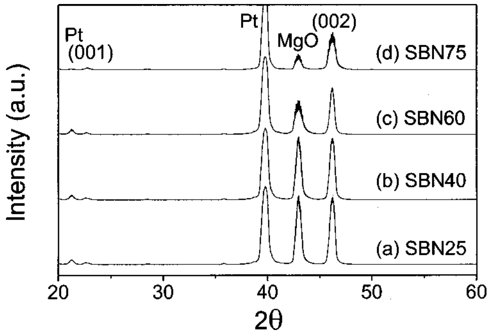

FIG. 1. XRD patterns of SBN thin films on Pt(100)/MgO(100) substrates as a function of film composition; (a) SBN25, (b) SBN40, (c) SBN60, and (d) SBN75.

$$\delta\phi_{2sp} \approx \left(\frac{2\pi d r_e E_m}{\lambda}\right)\left[\frac{n^2 \sin^2\theta}{(n^2-\sin^2\theta)^{1/2}}\right], \quad (2)$$

where $r_e = r_{33} - (n_o/n_e)^3 r_{13} \approx r_{33} - r_{13}$ is the effective electro-optic coefficient and $n \approx n_o \approx n_e$. The experimental setup for determination of the electro-optic coefficients of thin films is presented in Fig. 2. After reflection from the Pt electrode, the beam is separated into *p*- and *s*-polarized beams by a polarizing beam splitter (PBS). Then, after reflection from mirrors, a servo mirror, and a nonpolarizing beam splitter (BS), these beams are projected onto the photodiode where they mix again. Servo mirror with a feedback system was used for moving and stabilization of the operation point of TBP interferometer. The incident and polarization angles were set at 45°. The electric field $E = V/d = E_0 + E_m \sin(\omega t)$ was applied in the perpendicular direction to the plane of the thin film. The output signal was measured with a lock-in amplifier at the excitation frequency. Only the Fabry–Perot (FP) interferometer signal, S^{FP}, was measured when the half-wave retardation plate was removed. This signal was temporally stable even without an operation point stabilization system, and servo mirror displacement did not influence the value of this signal. But, when the half-wave retardation plate is installed, the *s*- and *p*-polarized beams reflected from Pt and ITO (indium tin oxide) electrode surfaces begin to create interference patterns with the beams with same polarization. ITO (3000 Å) as a transparent dot-shape top electrode, was deposited on the film surface using rf sputtering. Moving the operation point of the TBP interferometer by means of servo mirror displacement, we set the operation point of the TBP interferometer in the center of the left or right operation branches. The difference between the TBP interferometer signal, S^{TBP}, and the FP interferometer signal, S^{FP}, gives the value of S^{2sp}.

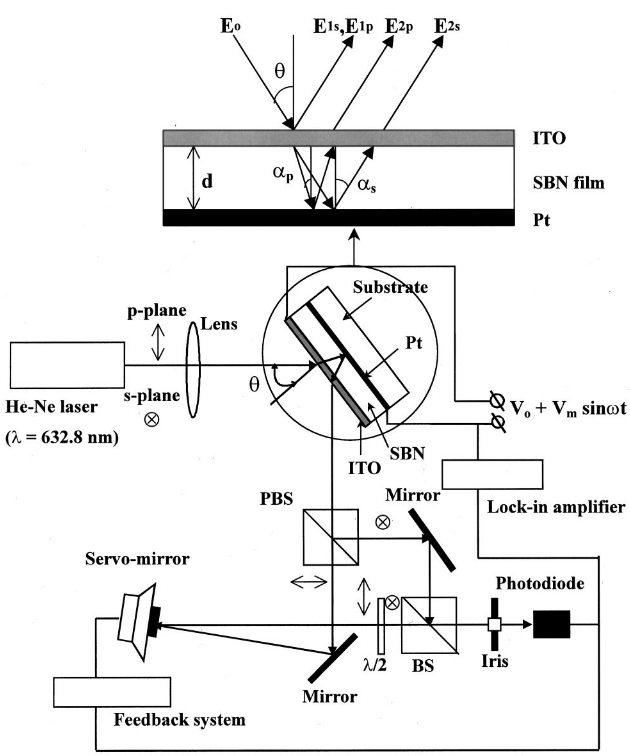

FIG. 2. Optical setup and detailed optical configuration for measurement of electro-optic coefficients of SBN thin films.

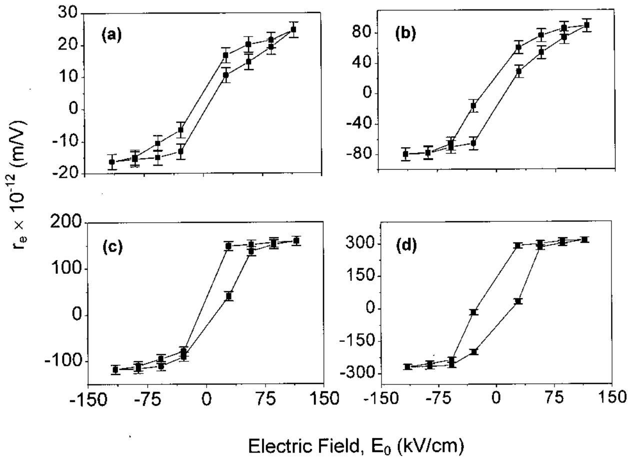

FIG. 3. Hysteresis loops of electro-optic coefficients for SBN thin films on Pt(100)/MgO(100) substrates as a function of film composition; (a) SBN25, (b) SBN40, (c) SBN60, and (d) SBN75.

$$S^{2sp} \approx S^{TBP} - S^{FP}. \quad (3)$$

Measurement of the output interferometer signals allows us to obtain the relationship between the measurement signals S^{2sp} and the real phase shift $\delta\phi_{2sp}$. Finally, the effective linear electro-optic coefficient, r_e, was estimated in Eqs. (2) and (3).

Figure 3 shows plots of the linear electro-optic coefficient (r_e) as a function of the dc electric field (E_0) which varies from −115 to 115 kV/cm with a fixed ac electric field ($E_m \approx 14$ kV/cm) and $\omega/2\pi$ (≈ 1 kHz). All the films show hysteresis with an asymmetric form, which may be due to the different materials used as top (ITO) and bottom (Pt) electrodes. Because of the asymmetric hysteresis loops, maximum electro-optic coefficients were calculated from the average in the following equation:

$$r_{e,\mathrm{avg}} = [(r_{e,\max}) + (-r_{e,\max})]/2. \quad (4)$$

The average maximum effective electro-optic coefficients of SBN25, 40, 60, and 75 thin films on MgO substrates were measured as 20.5, 84.3, 138.7, and 291.6 pm/V, respectively. Values of the electro-optic coefficient, r_{33} are estimated by assuming that the ratio of $r_{33}/r_{13} \approx 5$ and 20 for SBN60 and SBN75, respectively, as for bulk crystals.[9,13] Unfortunately, the ratios for the SBN25 and SBN40 crystals could not be found. Therefore, the magnitude of r_{33} for the SBN60 and

SBN75 thin films only are calculated to be approximately 173.4 and 306.9 pm/V, respectively. The effective electro-optic coefficient of the film increases as the Sr content in the film increases. This behavior originates from the linear electro-optic coefficient which is dependent on the spontaneous polarization and the dielectric constant.[14] Both P_s and ε values of SBN films are known to increase as the Sr content increases.[10] These values are smaller than those of single crystals (≈41, 205, 420, and 1300 pm/V for SBN25, 50, 60, and 75, respectively) and the films obtained by the PLD technique (≈350 and 844 pm/V for SBN60 and 75, respectively).[3,4,8,9] The smaller values in the sol-gel derived films may be caused by (a) the built-in strain in the film from thermal history and/or lattice mismatch between the film and the MgO substrate, or (b) lower quality of orientation caused by difficulty of crystallization control in the sol-gel processing. However, even the SBN25 thin film exhibits a larger value than that of $LiNbO_3$ crystal ($r_e = 18.9\,\mathrm{pm/V}$).[4]

In conclusion, we have prepared highly *c*-axis oriented SBN thin films on Pt(100)/MgO(100) substrates with various compositions using a sol-gel method. The electro-optic coefficients of these films were measured by a new experimental technique using a TBP interferometer. Since the sol-gel method enables the fabrication of microdevices with varied and complex shapes, sol-gel derived SBN thin films with large electro-optic coefficients measured in this study could be important for opto-electronic applications.

This work has been supported by the Korea Science and Engineering Foundation (Grant No. 981-0803-019-2).

[1] A. M. Glass, J. Appl. Phys. **40**, 4699 (1969).
[2] Y. Xu and J. D. Mackenzie, Integr. Ferroelectr. **1**, 17 (1992).
[3] P. V. Lenzo, E. G. Spencer, and A. A. Ballman, Appl. Phys. Lett. **11**, 23 (1967).
[4] Y. Xu, *Ferroelectric Materials and Their Applications* (Elsevier, Amsterdam, The Netherlands, 1991), pp. 81–85.
[5] A. Y. Wu, F. Wang, C. Juang, and C. Bustamante, Mater. Res. Soc. Symp. Proc. **200**, 261 (1990).
[6] S. S. Thöny, K. E. Youden, J. S. Harris, Jr., and L. Hesselink, Appl. Phys. Lett. **65**, 2018 (1994).
[7] S. Hirano, T. Yogo, K. Kikuta, and K. Ogiso, J. Am. Ceram. Soc. **75**, 1697 (1992).
[8] D. Trivedi, P. Tayebati, and M. Tabat, Appl. Phys. Lett. **68**, 3227 (1996).
[9] P. Tayebati, D. Trivedi, and M. Tabat, Appl. Phys. Lett. **69**, 1023 (1996).
[10] J. Koo, J. H. Jang, and B-S. Bae, J. Sol-Gel Sci. Technol. (to be published).
[11] W. Sakamoto, T. Yogo, K. Kikuta, K. Ogiso, A. Kawase, and S. Hirano, J. Am. Ceram. Soc. **79**, 2283 (1996).
[12] V. V. Spirin, C. Lee, and K. No, J. Opt. Soc. Am. B **15**, 1940 (1998).
[13] S. Ducharme, J. Feinberg, and R. R. Neurgaonkar, IEEE J. Quantum Electron. **QE-23**, 12 (1987).
[14] P. Gunter, *Electro-Optic and Photo-Refractive Materials* (Spinger, New York, 1991).